Photosynth Res (2016) 129:279–290
DOI 10.1007/s11120-016-0267-5

ORIGINAL ARTICLE

Photorespiration provides the chance of cyclic electron flow to operate for the redox-regulation of P700 in photosynthetic electron transport system of sunflower leaves

Daisuke Takagi[1] · Masaki Hashiguchi[1] · Takehiro Sejima[1] · Amane Makino[2] · Chikahiro Miyake[1]

Received: 24 November 2015 / Accepted: 18 April 2016 / Published online: 26 April 2016

Abstract To elucidate the molecular mechanism to oxidize the reaction center chlorophyll, P700, in PSI, we researched the effects of partial pressure of O_2 (pO_2) on photosynthetic characteristic parameters in sunflower (*Helianthus annuus* L.) leaves. Under low CO_2 conditions, the oxidation of P700 was stimulated; however the decrease in pO_2 suppressed its oxidation. Electron fluxes in PSII [Y(II)] and PSI [Y(I)] showed pO_2-dependence at low CO_2 conditions. H^+-consumption rate, estimated from Y(II) and CO_2-fixation/photorespiration rates (JgH^+), showed the positive curvature relationship with the dissipation rate of electrochromic shift signal (V_H^+), which indicates H^+-efflux rate from lumen to stroma in chloroplasts. Therefore, these electron fluxes contained, besides CO_2-fixation/photorespiration-dependent electron fluxes, non-H^+-consumption electron fluxes including Mehler-ascorbate peroxidase (MAP)-pathway. Y(I) that was larger than Y(II) surely implies the functioning of cyclic electron flow (CEF). Both MAP-pathway and CEF were suppressed at lower pO_2, with plastoquinone-pool reduced. That is, photorespiration prepares the redox-poise of photosynthetic electron transport system for CEF activity as an electron sink. Excess Y(II), [ΔY(II)] giving the curvature relationship with V_H^+, and excess Y(I) [ΔCEF] giving the difference between Y(I) and Y(II) were used as an indicator of MAP-pathway and CEF activity, respectively. Although ΔY(II) was negligible and did not show positive relationship to the oxidation-state of P700, ΔCEF showed positive linear relationship to the oxidation-state of P700. These facts indicate that CEF cooperatively with photorespiration regulates the redox-state of P700 to suppress the over-reduction in PSI under environmental stress conditions.

Keywords Cyclic electron flow · Electron sink · Mehler-ascorbate peroxidase (MAP)-pathway · Oxygen · Photosystem I · Photorespiration · P700

Abbreviations

AEE	Alternative electron flow
AL	Actinic light
APX	Ascorbate peroxidase
CEF	Cyclic electron flow
Chl	Chlorophyll
Ci	Partial pressure of intercellular CO_2
Cyt	Cytochrome
ΔpH	H^+-gradient across the thylakoid membranes
ECS	Electrochromic shift
ETR	Electron transport rate
JgH^+	H^+-consumption rate estimated from Y(II) and CO_2-fixation/photorespiration rate
MAP	Mehler-ascorbate peroxidase
NPQ	Non-photochemical quenching
P700	Reaction center P700 chlorophyll in PSI
PET	Photosynthetic electron transport

Daisuke Takagi and Masaki Hashiguchi have contributed equally to this work.

Electronic supplementary material The online version of this article (doi:10.1007/s11120-016-0267-5) contains supplementary material, which is available to authorized users.

✉ Chikahiro Miyake
cmiyake@hawk.kobe-u.ac.jp

[1] Department of Biological and Environmental Science, Faculty of Agriculture, Graduate School of Agricultural Science, Kobe University, 1-1 Rokkodai, Nada, Kobe 657-8501, Japan

[2] Department of Applied Plant Science, Graduate School of Agricultural Science, Tohoku University, Tsutsumidori-Amamiyamachi, Aoba-ku, Sendai 981-8555, Japan

PQ	Plastoquinone
PQH_2	Plastoquinol
PS	Photosystem
ROS	Reactive oxygen species
SOD	Superoxide dismutase
V_H^+	H^+-efflux rate estimated from ECS signal
Y(I)	Quantum yield of PSI
Y(II)	Quantum yield of PSII
Y(NA)	Quantum yield of non-photochemical quenching due to the acceptor-side limitation in PSI
Y(ND)	Quantum yield of non-photochemical quenching due to the donor-side limitation in PSI
pCO_2	Partial pressure of CO_2
pO_2	Partial pressure of O_2
qL	The fraction of oxidized Q_A
rSP	Repetitive short pulse
vc	RuBP carboxylation rate
vo	RuBP oxygenation rate

Introduction

Stagnation of photosynthesis induced by environmental stress causes electrons to accumulate in photosynthetic electron transport (PET) system (Asada 1999). For example, under high-light intensity, the supply of photon energy to PET system is in excess against the usage of photons to produce NADPH and ATP for CO_2 fixation (Kramer and Evans 2011). Furthermore, drought stress suppresses CO_2 fixation in the Calvin cycle by inducing stomata closure, which impedes the influx of CO_2 into leaves. In consequence, the decrease in partial pressure of intercellular CO_2 (Ci) in the leaves lowers the carboxylation activity of ribulose-1,5-bisphosphtae (RuBP) by RuBP carboxylase/oxygenase (Rubisco) (von Caemmerer and Farquhar 1981). The lower carboxylation rate of RuBP also induces the excess state of photon-energy supply to PET system even under low-light conditions. These lower efficiencies of photon usage induce the accumulation of electrons in PET system, which suffers from oxidative damages by reactive oxygen species (ROS) (Krieger-Liszkay 2005; Krieger-Liszkay et al. 2011; Roach and Krieger-Liszkay 2014).

Recently, we found that ROS produced in photosystem (PS) I of thylakoid membranes inactivates PSI itself in vivo and in vitro (Sejima et al. 2014; Takagi et al. 2016). To fulfill electrons in PET system, we repetitively illuminated short-pulse illumination to intact leaves of sunflower plants, and isolated chloroplasts from spinach leaves. Subsequently, we found that only in the presence of O_2, the repetitive short-pulse (rSP) treatment inactivates PSI, but not PSII (Sejima et al. 2014; Zivcak et al. 2015a, b; Takagi et al. 2016). The inactivation of PSI accompanied with the decreases in both oxidizable P700 content and CO_2 fixation activity, which indicated that ROS produced in PSI inhibited the charge separation of P700 and impaired PET reaction (Sejima et al. 2014; Zivcak et al. 2015a; Takagi et al. 2016). About PSI photoinhibition induced by rSP treatment, we found that ROS scavenging system consisted with Cu–Zn superoxide dismutase (SOD) and ascorbate peroxidase (APX) cannot protect PSI from its photoinhibition (Takagi et al. 2016). On the other hand, we also found that oxidation of P700 suppressed the inactivation of PSI activity (Sejima et al. 2014). In Sejima et al. (2014), we regulated the redox-state of P700 by illuminating actinic light (AL) to intact leaves during the rSP treatment. Then, PSI photoinhibition was suppressed with the increase in oxidized P700. That is, stimulating the formation of oxidized P700 is important in order to escape ROS production in PSI and PSI photoinhibition (Sejima et al. 2014; Takagi et al. 2016).

In higher plants, the increase in oxidized P700 on exposure to high light and low-[CO_2] is observed (Golding and Johnson 2003; Miyake et al. 2005). This would be the regulative response of PET system to suppress ROS production in PSI under such stressful conditions. In fact, mutants of *Arabidopsis thaliana* which was deficient in the activity of Fd-dependent increase in minimal Chl fluorescence (*pgr5* mutant), or state-transition (*stn7* mutant) did not show the induction of oxidized P700 under fluctuating light conditions (Grieco et al. 2012; Suorsa et al. 2012; Kono et al. 2014), and suffered from PSI photoinhibition. These mutants underwent the accumulation of electrons in PET system, which would produce ROS (Suorsa et al. 2012; Tikkanen et al. 2012; Tikkanen and Aro 2014).

Several candidates for the molecular mechanism to oxidize P700 have been proposed (Miyake 2010). For the oxidation of P700, two aspects should be considered; first, electron sink in photosynthesis to consume electrons produced in PET system; second, limitation of electron flow to P700 from PSII. As an electron sink which alternates to CO_2 fixation, photorespiration would have potential to consume electrons (Brestic et al. 1995; Kozaki and Takeba 1996; Badger et al. 2000; von Caemmerer 2000; Sejima et al. 2016). The electron flow to P700 is regulated by acidification of the lumenal side of thylakoid membranes (Schreiber and Neubauer 1990; Heber and Walker 1992; Kramer et al. 1999; Miyake 2010; Johnson 2011; Tikhonov 2013). Mehler-ascorbate peroxidase (MAP) pathway (the water–water cycle) and cyclic electron flow around PSI (CEF) can induce the acidification of lumenal side of thylakoid membranes, which drive non-photochemical quenching (NPQ) of Chl fluorescence to decrease excitation efficiency of PSII, and suppress the PQH_2-oxidation activity in Cyt b_6f-complex (Miyake 2010). Therefore, MAP-pathway and CEF would trigger the slowing down of

the electron flow to P700 in PSI from PSII owing to the acidification of lumenal side of thylakoid membranes. The electron flows alternate to CO_2 fixation is called "alternative electron flow (AEF)," which includes photorespiration, MAP-pathway, and CEF.

In the present work, we aimed to elucidate the oxidation mechanism of P700 in leaves of sunflower (*Helianthus annuus* L.), and to determine which pathway or pathways among photorespiration, MAP-pathway, or CEF controls the oxidation level of P700. Both photorespiration and MAP-pathway require O_2 to express their activities. However, MAP-pathway does not consume ATP. Thus, we can distinguish H^+-consumption pathway, photorespiration, from MAP-pathway by analyzing electrochromic shift (ECS)-signal, which indicates ATP synthesis activity during photosynthesis (Kanazawa and Kramer 2002; Avenson et al. 2005; Takizawa et al. 2008; Sejima et al. 2016). We studied the effects of partial pressure of O_2 on PET system, and found that photorespiration contributes to the oxidation of P700, and prepares the redox-poise in PET system for CEF turnover, which supports to oxidizing P700 in PSI.

Materials and methods

Plant materials

In this study, we used sun flower (*Helianthus annuus* L.) as a plant material. Seeds were imbibed using wet cotton at 4 °C for 3 days to promote synchronized germination. The imbibed seeds were grown in a mixture of soil (Metro-Mix 350; Sun Gro Horticulture, Bellevue, WA, USA) and vermiculite (Konan, Osaka, Japan) in pots (12 × 12 cm^2 in width and 9.5 cm in depth). The plants were placed in an environmentally controlled chamber with 14 h of light (25 °C) and 10 h of darkness (23 °C). The light intensity was 500 μE m^{-2} s^{-1}. The seedlings were watered every second day with 0.1 % Hyponex solution (N:P:K = 5:10:5, Hyponex, Osaka, Japan). Analyses were carried out on fully expanded mature leaves of plants grown for at least 4 weeks.

Gas exchange analysis and measurement of chlorophyll fluorescence and $P700^+$

For correct understanding of photosynthesis in higher plants, we measured gas exchange analysis, chlorophyll fluorescence, and $P700^+$ simultaneously with a Li-7000 (Li-Cor, Nebraska, USA) and Dual-PAM-100 (Heintz Walz GmbH, Effeltrich, Germany). In this measurement, we used a 3010 DUAL gas exchange leaf chamber (Heintz Walz GmbH, Effeltrich, Germany). Atmospheric gas (40 Pa CO_2/21 kPa O_2) and gas with the indicated mixture of pure O_2 and CO_2 were prepared by mixing 20.1 % (v/v) O_2 in 79.9 % (v/v) N_2, 1 % (v/v) CO_2 in 99 % N_2, and pure N_2 gas using a mass-flow controller (Kofloc model 1203; Kojima Instrument Co., Kyoto, Japan). The gases were saturated with water vapor at 18.0 ± 0.1 °C and the leaf temperature was maintained at 25 °C. The chlorophyll fluorescence parameters were calculated as follows (Kramer et al. 2004; Baker 2008; Miyake et al. 2009): maximum quantum efficiency of PSII photochemistry, $Fv/Fm = (Fm - Fo)/Fm$; quantum yield of photochemical energy conversion in PSII, $Y(II) = (Fm' - Fs)/Fm'$; non-photochemical quenching $NPQ = (Fm - Fm')/Fm'$; Q_A oxidized state $(qL) = (Fm' - Fs)/(Fm' - Fo') \times (Fo'/Fs)$; Fo, minimum fluorescence yield; Fm, maximum fluorescence yield; and Fs, steady-state fluorescence yield. Measuring light (0.1 μE m^{-2} s^{-1}) and saturated pulse (20,000 μE m^{-2} s^{-1}, 300 ms) were applied to determine Fo and Fm. H^+-consumption rate (JgH^+) estimated from CO_2 fixation rate (A), respiration rate (Rd), and electron transport rate (ETR) was calculated as described in Sejima et al. (2016), on the assumption that MAP-pathway did not function as AEF. For this calculation, RuBP carboxylation rate (vc) and RuBP oxygenation rate (vo) were calculated as follows: $vc = (1/6) \times \{ETR - 4 \times (A + Rd)\}$, $vo = (1/6) \times \{ETR/2 + 4 \times (A + Rd)\}$. In this study, ETR was calculated, as follows: $ETR = AL\ intensity \times Y(II) \times 0.45$. By using these parameters, JgH^+ was calculated, as follows: $JgH^+ = 9.34 \times (vc + vo) \times \{3 + 3.5 \times (vo/vc)\}/\{2 + 2 \times (vo/vc)\}$ (Sejima et al. 2016). The oxidation–reduction state of $P700^+$ was determined according to the methods of Klughammer and Schreiber (1994) as follows: quantum yield of photochemical energy in PSI, $Y(I) = (Pm' - P)/Pm$; quantum yield of non-photochemical quenching due to the acceptor-side limitation, $Y(NA) = (Pm - Pm')/Pm$; and quantum yield of non-photochemical quenching due to the donor-side limitation, $Y(ND) = P/Pm$. The maximum oxidation level of P700 chlorophyll (Pm) was obtained by a saturated pulse under far-red light and reflected the maximum amount of photooxidized P700 chlorophyll. The parameter P reflects the steady-state oxidation level of $P700^+$, and Pm' was obtained by a saturated pulse at a steady state. Actinic red light (AL) was used to measure the photosynthetic parameters.

Measurement of electrochromic shift

Gas exchange analysis and electrochromic shift were simultaneously measured with a Li-7000 and Dual-PAM which equipped with P515-analysis module (Klughammer et al. 2013). Gaseous phase was controlled as described in the method of gas exchange analysis and measurement of

chlorophyll fluorescence and $P700^+$. The gases were saturated with water vapor at 18.0 ± 0.1 °C and the leaf temperature was maintained at 25 °C. The *proton motive force*, proton conductance (gH^+) in ATPsynthase, and H^+ efflux rate (V_H^+) was measured by dark-interval relaxation kinetics (DIRK) analysis as described in (Sacksteder and Kramer 2000; Baker et al. 2007). For the DIRK analysis, we set the transient dark (600 ms) during AL illumination. In this analysis, we measured the extend of the change in ECS as a *proton motive force*, and the half-life ($\tau_{1/2}$) of ECS decay for the calculation of gH^+ ($1/\tau_{1/2}$). V_H^+ was estimated from the initial decay of ECS during the transient dark. The value of *proton motive force* was normalized by dividing the magnitude of ECS decay in DIRK analysis on the magnitude of ECS induced by single turnover flash (10 μs) (Klughammer et al. 2013).

Results and discussion

We aimed to elucidate what molecular mechanism regulates the oxidation level of P700 [Y(ND)] in PSI of thylakoid membranes. As described in introduction, the electron sink and the limitation of electron flow to P700 could control Y(ND). We studied the effects of pO_2 on photosynthesis characteristics in sunflower leaves, because photorespiration requires O_2 to function as an electron sink, and MAP-pathway also requires O_2 to induce ΔpH across thylakoid membranes. Simultaneously, we tried to evaluate CEF activity from the difference between Y(I) and Y(II) (Kou et al. 2013, 2015).

Effects of pO_2 on photosynthetic CO_2-fixation in sunflower leaves

At 40 Pa of the partial pressure of CO_2 (pCO_2), pO_2 decreased from 21 to 0 kPa after photosynthetic CO_2 fixation rate reached the steady state (Fig. 1). With lowering pO_2, CO_2 fixation rate increased from 16 to 23 μmol CO_2 m^{-2} s^{-1}. This was due to the suppression of photorespiration activity (von Caemmerer 2000). At 4 Pa of pCO_2, CO_2 fixation rate was lower than that at 40 Pa of pCO_2 and 21 kPa of pO_2. This is because lower pCO_2 suppressed CO_2 fixation rate to near zero, where Ci was close to CO_2-compensation point. At 4 Pa of pCO_2, photorespiration activity was also suppressed with lowering pO_2, as observed in the increase in CO_2 fixation rate to about 2 μmol CO_2 m^{-2} s^{-1}.

Effects of pO_2 on parameters of PSII

At 40 Pa of pCO_2, Y(II) and qL almost did not respond to the decrease in pO_2 (Fig. 2a, b). This would be due to a reason that photosynthetic CO_2 fixation was not limited by Rubisco (Miyake et al. 2005). At 4 Pa of pCO_2, Y(II) was lower than that at 40 Pa of pCO_2. This would be due to the lower photosynthetic CO_2 fixation rate (Fig. 1). Y(II) decreased with lowering pO_2 from 10 kPa (Fig. 2a). This would be mainly due to the suppression of photorespiration, as observed in Fig. 1. qL at 4 Pa pCO_2 was also lower than that at 40 Pa of pCO_2, and qL decreased with lowering pO_2 from 10 kPa (Fig. 2b). The behavior of qL resembled Y(II) (Fig. 2a). These facts suggest that photorespiration functioned as an electron sink to oxidize plastoquinone (PQ)-pool under CO_2 limited conditions. NPQ was higher at 4 Pa of pCO_2 than that at 40 Pa of pCO_2, and NPQ decreased with lowering pO_2 from 2 kPa (Fig. 2c). These results suggest the induction of *proton motive force* during the limitation of CO_2 fixation, as observed in the increase in NPQ.

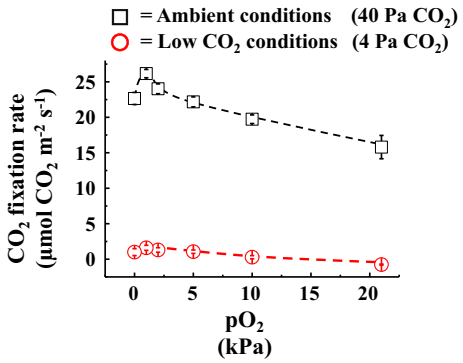

Fig. 1 pO_2 response of CO_2 fixation rate in leaves. Before this analysis, plants were pre-illuminated at growth light intensity (500 μE m^{-2} s^{-1}) under ambient conditions [Partial pressure of CO_2 (pCO_2) 40 Pa, pO_2 21 kPa, 25 °C] for activating electron sink. After the electron sink activation, pO_2 concentration was decreased in phase from 21 to 0 kPa. For each pO_2, the parameters were obtained at steady state. *Black square*, leaves under 40 Pa pCO_2; *Red circle*, leaves under 4 Pa pCO_2; Data were expressed as mean ± SEM of three independent experiments

Effects of pO_2 on parameters of PSI

At 40 Pa of pCO_2, Y(I), Y(ND), and Y(NA) almost did not respond to the decrease in pO_2 (Fig. 3). This would be due to a reason that photosynthetic CO_2 fixation was not limited by Rubisco, as observed in Y(II) (Fig. 2a) (Miyake et al. 2005). At 4 Pa of pCO_2, Y(I) was lower than that at 40 Pa of pCO_2, and Y(I) decreased with lowering pO_2 from 10 kPa (Fig. 3a). These responses of Y(I) resembled those of Y(II) (Fig. 2a). Y(ND) at 4 Pa pCO_2 was higher than that at 40 Pa of pCO_2, and Y(ND) decreased with lowering pO_2 from 10 kPa (Fig. 3b). The behavior of Y(ND) at 4 Pa pCO_2 resembled Y(I) at 4 Pa pCO_2 (Fig. 3a). Y(NA) at 4 Pa pCO_2 was the same with that at 40 Pa of pCO_2 when O_2 adequately exists, however Y(NA) at 4 Pa pCO_2

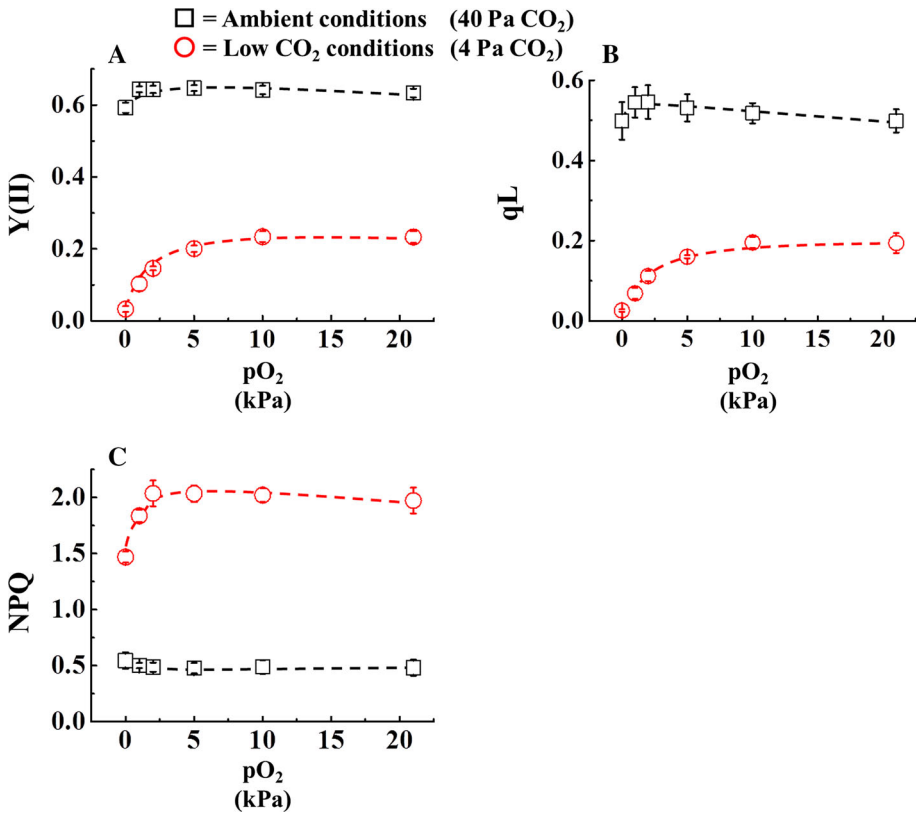

Fig. 2 pO_2 response of Y(II) (**a**), qL (**b**), and NPQ (**c**). Before this analysis, plants were pre-illuminated at growth light intensity (500 μE m^{-2} s^{-1}) under ambient conditions (pCO_2 40 Pa, pO_2 21 kPa, 25 °C) for activating electron sink. After the electron sink activation, pO_2 concentration was decreased in phase from 21 to 0 kPa. For each pO_2, the parameters were obtained at steady state. *Black square*, leaves under 40 Pa pCO_2; *Red circle*, leaves under 4 Pa pCO_2. Data were expressed as mean ± SEM of three independent experiments

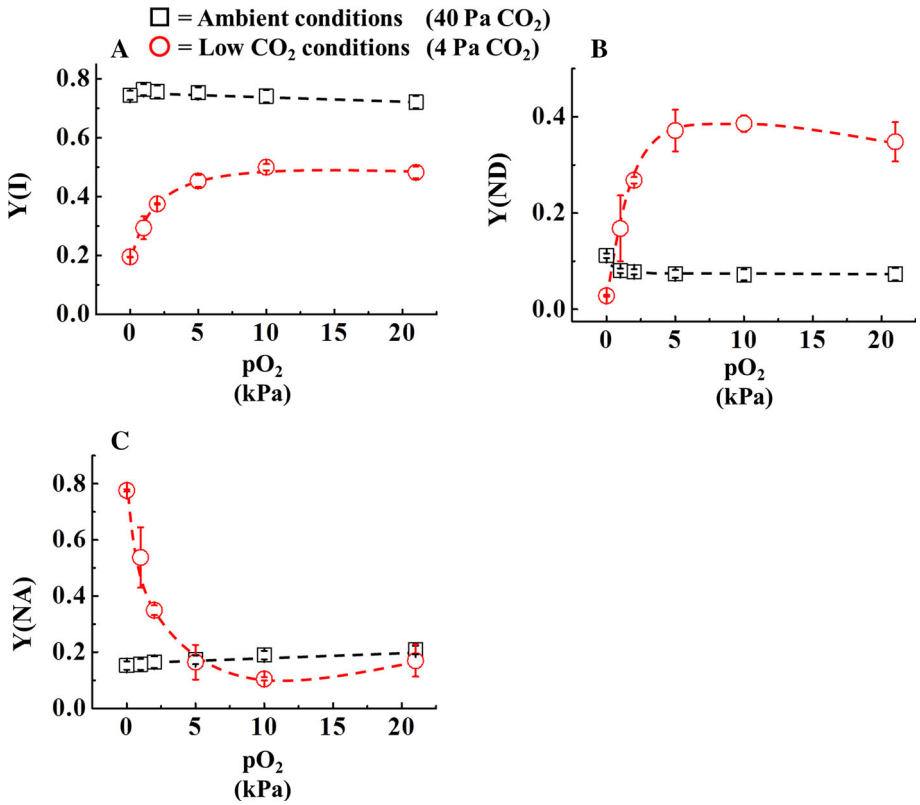

Fig. 3 pO_2 response of Y(I) (**a**), Y(ND) (**b**), and Y(NA) (**c**). Before this analysis, plants were pre-illuminated at growth light intensity (500 μE m^{-2} s^{-1}) under ambient conditions (pCO_2 40 Pa, pO_2 21 kPa, 25 °C) for activating electron sink. After the electron sink activation, pO_2 concentration was decreased in phase from 21 to 0 kPa. For each pO_2, the parameters were obtained at steady state. *Black square*, leaves under 40 Pa pCO_2; *Red circle*, leaves under 4 Pa pCO_2. Data were expressed as mean ± SEM of three independent experiments

increased with lowering pO_2 from 10 kPa (Fig. 3c). At 4 Pa pCO_2, the behavior of Y(NA) was reverse to Y(I) and Y(ND) (Fig. 3a, b). These results indicate that, at 4 Pa pCO_2, the decrease in Y(I) with lowering pO_2 is caused by the limitation of acceptor-side in PSI. On the basis of these results, P700 is oxidized depending on the presence of O_2 when CO_2 fixation is suppressed. That is, photorespiration contributes to the oxidation of P700, which suppresses the limitation of acceptor-side of P700. For the induction of Y(ND), slowing down of photosynthetic electron flow from PSII to PSI would be required, and then ΔpH across the thylakoid membranes critically contributes to the limitation of electron flux to PSI (Tikhonov 2013). Therefore, photorespiration should involve in the formation of *proton motive force* under CO_2 limited conditions. In the next chapter, we studied the formation mechanism of *proton motive force* under CO_2 limited conditions.

Effects of pO_2 on H^+-consumption rate

AEF including MAP-pathway and CEF do not consume H^+ accumulated in lumenal side of thylakoid membranes during CO_2 fixation and photorespiration. To elucidate the molecular mechanisms of AEF to induce Y(ND), we studied the dependence of electron flux in both PSII and PSI on H^+-consumption rate.

At 40 Pa of pCO_2, *proton motive force* almost did not respond to the decrease in pO_2 (Fig. 4a). This would be due to the constant electron fluxes in both PSII and PSI (Figs. 2a, 3a). At 4 Pa of pCO_2, *proton motive force* was larger than that at 40 Pa of pCO_2, even though photosynthesis decreased (Figs. 2a, 3a). For the formation of *proton motive force*, PET reaction is required. That is, the decrease in electron sink of CO_2 fixation activated AEF which induces *proton motive force*. The *proton motive force* decreased with lowering pO_2 (Fig. 4a). This would be due to the suppressions of AEF including photorespiration, MAP-pathway, and CEF. H^+-conductance (gH^+) almost did not respond to the decrease in pO_2 at 40 Pa pCO_2 (Fig. 4b). In contrast, at 4 Pa of pCO_2, gH^+ was lower than that at 40 Pa of pCO_2, and gH^+ decreased with lowering pO_2 (Fig. 4b). H^+-consumption rate (V_H^+) almost did not respond to the decrease in pO_2, except that below 2 kPa pO_2 at 40 Pa pCO_2 (Fig. 4c). At 4 Pa of pCO_2, V_H^+ was lower than that at 40 Pa of pCO_2, and V_H^+ decreased with lowering pO_2 (Fig. 4c). gH^+ and V_H^+ is determined by the H^+-efflux activity through ATPsynthase to generate ATP from ADP, and Pi (Baker et al. 2007; Takizawa et al. 2008). That is, the change in gH^+ and V_H^+ means the change of availability of ADP and Pi in chloroplast (Kanazawa and Kramer 2002; Avenson et al. 2005; Takizawa et al. 2008). Therefore, this result showed that the turnover rate of ATP to produce ADP and Pi decreases with lowering pO_2. Based on these observations, we suggested that H^+-consuming O_2-dependent photosynthetic electron flow, namely photorespiration, is exactly driven at 4 Pa pCO_2 as a main AEF, but not MAP-pathway which does not consume ATP (Sejima et al. 2016).

To confirm whether all the AEF activity depending on O_2 can be explained by the activity of photorespiration, we studied the relationship between ATP consumption rate, which was estimated from CO_2 fixation and photorespiration, and V_H^+. ATP consumption rate is expressed as JgH^+, which depends on the rates of RuBP carboxylase and oxygenase activities (*vc* and *vo*; see "Materials and methods," Sejima et al. 2016). First, we assumed that MAP-pathway did not function in the estimation of JgH^+ from the values of Y(II) and the net CO_2 assimilation rate. If MAP-pathway functioned, Y(II) would be overestimation due to the electron flow driven by MAP-pathway. JgH^+ was plotted against V_H^+, which was estimated from ECS-analysis in vivo (Sejima et al. 2016). Contrary to our expectations, JgH^+ behaved as curvature fashion against V_H^+ (Fig. 5a). On the other hand, JgH^+ had a positive linear relationship with Y(II) (Supplemental Fig. S1). These results indicate that Y(II) used for the evaluation of JgH^+ involves electron flux of AEF, which does not consume H^+, in addition to photorespiration-dependent electron flux. In fact, Y(II) clearly shows the deviation (indicated by shade area) from the positive linear relationship between Y(II) and V_H^+ (Fig. 5b). The deviation shows the presence of AEF, which requires O_2 to express its activity. The most plausible candidate mechanism to drive this AEF is MAP-pathway.

We found that Y(I) was larger than Y(II), and Y(I) also shows the deviation from the linear relationship between Y(I) and V_H^+ (Fig. 5c). Y(I) also showed the dependence on pO_2 (Fig. 3a). These results show that Y(I) involves the electron fluxes for photorespiration and MAP-pathway as photosynthetic linear electron flow and CEF.

To elucidate the molecular mechanism of AEF to induce Y(ND), we plotted Y(ND) against V_H^+ (Fig. 5d). With the decrease in V_H^+ from about 100–40 s^{-1}, Y(ND) increased, and then decreased. These results possess the possibility that the suppression of photorespiration lowered other AEF activity producing *proton motive force* under CO_2 limited conditions.

To confirm whether Y(ND) and *proton motive force* are induced by MAP-pathway and CEF under CO_2 limited conditions, we estimated their activity and studied the capability to oxidize P700. First, we plotted Y(ND) against *proton motive force* (Fig. 6a). Then, we confirmed the induction of Y(ND) required *proton motive force*. We calculated non-H^+-consumption electron flux in PSII, MAP-pathway activity, shown as the shaded area in Fig. 5b. Red linear line showed the electron flux in PSII

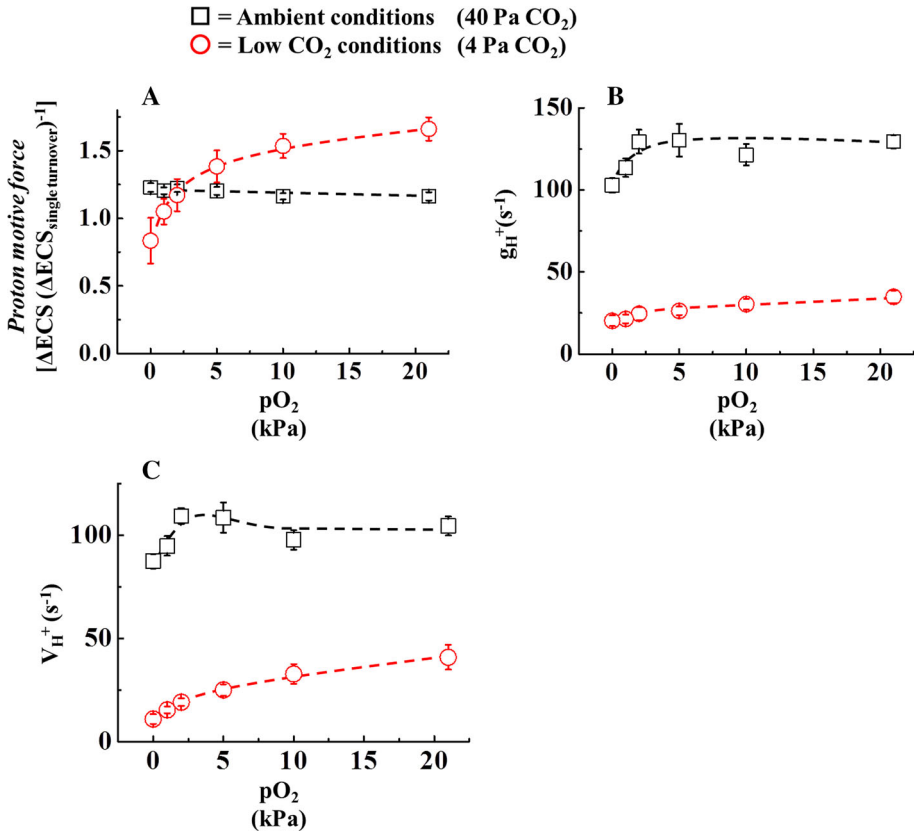

Fig. 4 pO_2 response of *proton motive force* (**a**), gH^+ (**b**), and V_H^+ (**c**). Before this analysis, plants were pre-illuminated at growth light intensity (500 μE m^{-2} s^{-1}) under ambient conditions (pCO_2 40 Pa, pO_2 21 k Pa,25 °C) for activating electron sink. After the electron sink activation, pO_2 concentration was decreased in phase from 21 to 0 kPa. For each pO_2, the parameters were obtained at steady state. *Black square*, leaves under 40 Pa pCO_2; *Red circle*, leaves under 4 Pa pCO_2. Data were expressed as mean ± SEM of three independent experiments

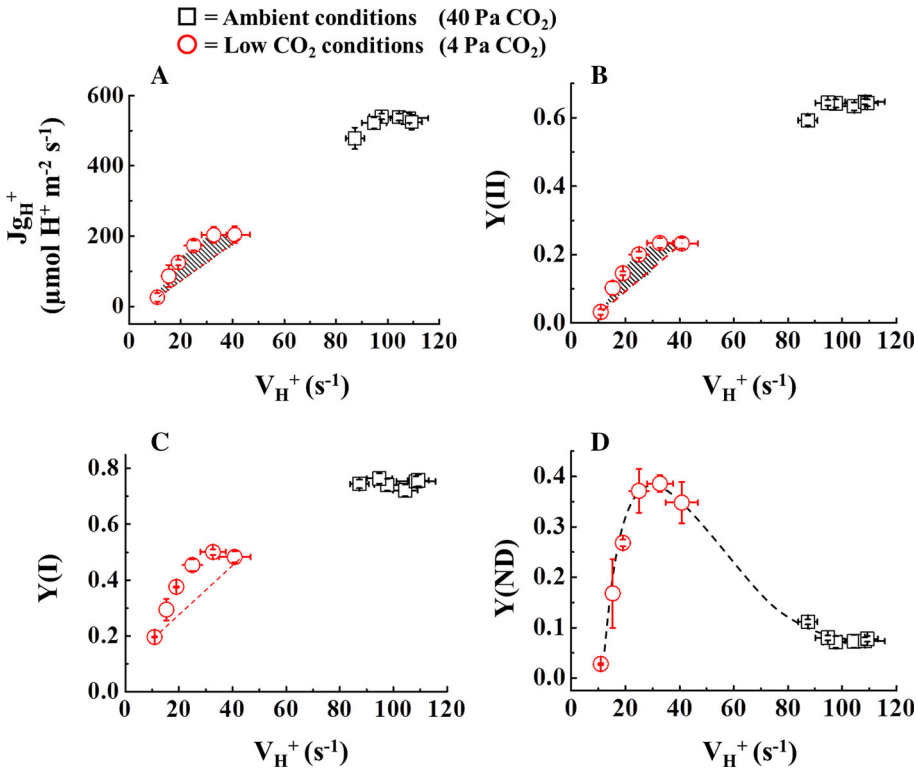

Fig. 5 The effect of H^+ consumption rate (V_H^+) estimated from ECS to JgH^+ (**a**), Y(II) (**b**), Y(I) (**c**), and Y(ND) (**d**) was shown. The values of V_H^+, Y(ND), and Y(II) were used in Figs. 2, 3, and 4. JgH^+ was also calculated from the value of CO_2 fixation rate and Y(II) presented in Figs. 1 and 2a. *Black square*, leaves under 40 Pa pCO_2; *Red circle*, leaves under 4 Pa pCO_2

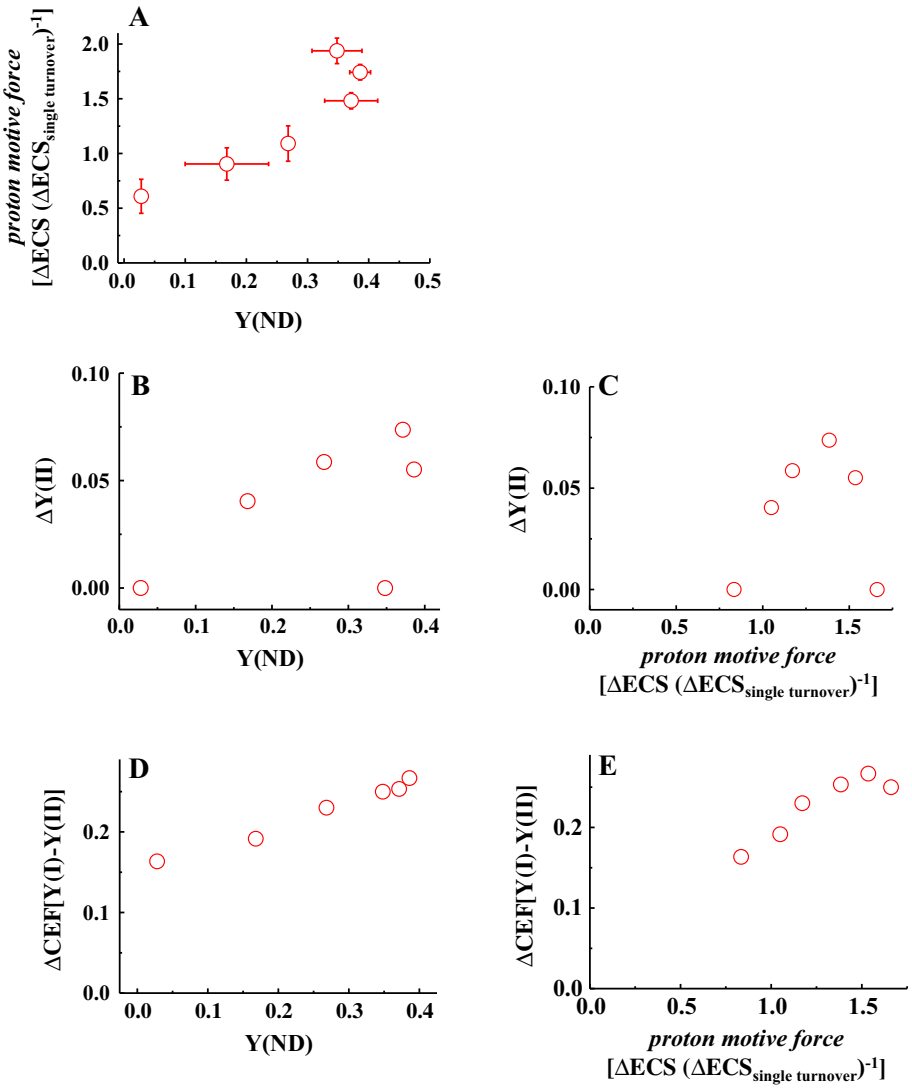

Fig. 6 The relationships between Y(ND) and *proton motive force* (**a**), ΔY(II) and Y(ND) (**b**), ΔY(II) and *proton motive force* (**c**), ΔCEF and Y(ND) (**d**), and ΔCEF and *proton motive force* (e) were shown. The values of Y(ND) were used in Fig. 3. The value of ΔY(I) was calculated by subtracting Y(II) from Y(I), which are shown in Figs. 2 and 3. The values of *proton motive force* were used in Fig. 4. *Red circles* indicate the data obtained at 4 Pa pCO_2

required for driving CO_2 fixation and photorespiration. The deviation of Y(II) from the red line showed the electron flux reflecting non-H^+-consumption electron flux. Subsequently, we found that there are no significant relationship between ΔY(II) and Y(ND), or ΔY(II) and *proton motive force* (Fig. 6b, c). These results indicate that MAP-pathway could not contribute to the formation of *proton motive force*, and the oxidation of P700.

Next, non-H^+-consumption electron flux in PSI, CEF activity (ΔCEF) was calculated from the difference between Y(I) and Y(II) (Kou et al. 2013, 2015). We plotted ΔCEF against Y(ND) and *proton motive force* (Fig. 6d, e). We found that ΔCEF showed positive linear relationship with Y(ND) and *proton motive force*. These data supported the idea that CEF contributes to the induction of *proton motive force* to induce Y(ND).

In the present research, we showed that photorespiration functioned as an electron sink, shown as the inductions of Y(II) and qL. That is, photorespiration oxidized PQ-pool (Figs. 1, 2). In addition, a decrease in qL accompanied the increase in Y(NA) (Fig. 3). These results suggest that photorespiration regulates the redox-state of PET system as an electron sink at lower CO_2 conditions. In concert with the activity of photorespiration, CEF contributes to the oxidation of P700. That is, CEF would require O_2 to prepare the redox-poise for driving CEF.

Concluding remarks

We succeeded in the elucidation of the physiological importance of photorespiration under CO_2 limited conditions. Furthermore, we also succeeded in the detection of AEF which does not consume H^+ accumulated in the lumenal side of thylakoid membranes by plotting both Y(I) and Y(II) against V_H^+. Our method is useful to evaluate the activities of CEF and MAP-pathway in vivo. From our present research, we confirm that CEF cooperatively

contributes to regulate the redox-state of P700 with the help of photorespiration, which stimulates the oxidation of electron carriers in PSI of thylakoid membranes.

CEF can drive the induction of ΔpH across thylakoid membranes, and contribute to the production of ATP (Heber and Walker 1992; Miyake et al. 1995). The concept of CEF was first proposed in Arnon 1959, and developed in Allen 2002, and Allen 2003. CEF story was made in in vitro experiments (Okegawa et al. 2008; Miyake et al. 1995; Munekage et al. 2002; Nishikawa et al. 2012; Shikanai 2007; Yamamoto et al. 2011; Yamamoto and Shikanai 2013; Wang et al. 2014). Recently, two molecular mechanisms to drive CEF were proposed using mutants of *Arabidopsis thaliana* by Shikanai's group (Yamamoto et al. 2011; Wang et al. 2014). Ferredoxin (Fd)-dependent PQ oxidoreductase (FQR)-pathway and NAD(P)H dehydrogenase like complex (NDH)-dependent pathway function in vivo (Munekage et al. 2008; DalCorso et al. 2008; Livingston et al. 2010; Yamori et al. 2015). FQR requires PGR5 protein, which activity is inhibited by the antibiotics antimycin A. NDH and PGR5-dependent CEF activities range from 0.035 s^{-1} in vitro (Fisher and Kramer 2014), 0.1 s^{-1} in vivo (Trouillard et al. 2012), to 1 s^{-1} in vivo (Gotoh et al. 2010). Although these activities are quite lower than the turnover rate of photosynthesis, PGR5-dependent CEF can induce *proton motive force*. In fact, Miyake et al. (1995), and Strand et al. (2016) observed that antimycin A-sensitive CEF induces *proton motive force* although the induction rate was also slow. In addition to antimycin A-sensitive pathway, NDH pathway is also capable to form *proton motive force* (Livingston et al. 2010). Importantly, under low CO_2 conditions, the demand on ATP synthesis rate for the Calvin cycle and photorespiration would be lower than ambient conditions because gH^+ was considerably lower at 4 Pa CO_2 than 40 Pa CO_2 (Fig. 4b) (Kanazawa and Kramer 2002; Takizawa et al. 2008; Kohzuma et al. 2009). Therefore, H^+-efflux from lumenal side to stromal side in chloroplasts is restricted at 4 Pa CO_2 than 40 Pa CO_2, and H^+ accumulation is accelerated (Fig. 4c). That is, even CEF is the minor flux of photosynthesis, its activity would be enough to induce *proton motive force*. Therefore, CEF activity, which was detected as ΔCEF to induce Y(ND), would contain both PGR5- and NDH-dependent CEF in vivo. Furthermore, CEF requires the optimum redox-state of PQ-pool to express its maximum activity (Hormann et al. 1994; Allen 2003). At the extreme, reduced and oxidized states of PQ-pool CEF cannot turnover and cannot induce *proton motive force*. Thus, CEF activity decreased with photorespiration activity, which suppresses the over-reduction of PET system.

Laisk et al. (2010) reported that intact leaves have two kinds of CEF: fast- and slow-types, respectively (Miyake 2010). The slow-type is driven by PGR5/NDH-dependent CEFs. The fast-type CEF does not induce *proton motive force*, and the molecular mechanism to drive fast-type CEF remains unknown. The turnover rate of fast-type CEF *in planta* is estimated about 70–200 s^{-1} per PSI (Joliot and Joliot 2002; Joliot et al. 2004; Laisk et al. 2007, 2010), which is much higher than NDH and PGR5-dependent CEF activities. The discrimination of fast- and slow-type CEFs would be difficult, because CEF requires the optimum redox-state, the redox-poise, to express their maximum activities. Therefore, their dependence on the redox-state of PQ-pool would be similar between fast- and slow-types. Thus, ΔCEF observed in the present research would contain the electron fluxes of both fast- and slow-type of CEF.

CEF to produce *proton motive force* is not required for photosynthesis (Nishikawa et al. 2012; Kou et al. 2013, 2015). Mutants deficient in PGR5-protein in rice and *Arabidopsis* plants show the same photosynthesis rate with wild-type plants (Nishikawa et al. 2012; Kou et al. 2013, 2015). Furthermore, even though the redox-state of P700 is hampered by antimycin A-treatment, photosynthesis rate is kept at the same rate with the non-treated state (Kou et al. 2015). These facts show that CEF does not contribute to driving photosynthesis, namely ATP synthesis. Although the electron flux of slow-type CEF is too small compared to photosynthesis electron flux, slow-type CEF can slowly load the *proton motive force* on which PET reaction induces. Therefore, physiological function of CEF would be to load *proton motive force* for the enhancement of the oxidation of P700, and the formation of NPQ to protect PET system from ROS damages, especially under CO_2 limited conditions.

MAP-pathway (the water–water cycle) can drive O_2-dependent electron flow in chloroplasts, which magnitude ranges from 10 to 40 μmol O_2 $(mg\ Chl)^{-1}\ h^{-1}$ (Asada et al. 1974; Furbank and Badger 1983; Heber et al. 1978; Hormann et al. 1994; Takahashi and Asada 1982, 1988). These values correspond to about 1 to 5 μmol O_2 $m^{-2}\ s^{-1}$ in intact leaves, which are close to those reported by Driver and Baker (Driever and Baker 2011). Although the electron flux driven by MAP-pathway occupies a minor flux of photosynthesis, MAP-pathway has potential to induce *proton motive force* and NPQ in vitro (Hormann et al. 1994; Schreiber et al. Schreiber and Neubauer 1990, Schreiber et al. 1991; Takagi et al. 2012). In contrast, we failed to find the induction of *proton motive force* and Y(ND) by non-H^+-consumption electron flux in PSII, which is estimated as the activity of MAP-pathway (Fig. 6b, c). Compared to ΔCEF, ΔY(II) showed smaller value (Fig. 6b–e). Therefore, the activity of MAP-pathway would be lower than CEF activity, and MAP-pathway might not contribute to any induction of *proton motive force* in vivo.

Recently, our research group found the new regulatory mechanism to oxidize P700 in PET system of the cyanobacterium *Synechococcus elongatus* PCC7942 (*S.* 7942) (Shaku et al. 2015). The deletion of flavodiiron protein-dependent Mehler reaction suppressed photosynthesis with PQ reduced, and enhanced oxidation of P700. Reduction of PQ-pool suppressed O_2-evolution rate, and oxidized NADPH, P700, and Cyt *f*, respectively (Shaku et al. 2015). Our research group calls this suppressed electron flow, which was brought by the reduction of PQ-pool, a reduction-induced suppression of electron flow "RISE." RISE contributes to oxidize electron carriers in PSI. In the present work, lowering CO_2 caused PQ-pool reduced, as observed in the decrease in qL with increase in Y(ND) (Figs. 2b, 3b). The presence and its physiological function of RISE in higher plants will be elucidated in the future.

Acknowledgments This work was supported by the Japan Society for the Promotion of Science [Scientific Research Grant No. 21570041 to C.M.]. The authors would like to thank Editage (Cactus Communications Inc., http://www.editage.jp/) for the English language review.

Compliance with ethical standards

Conflict of interest The authors have no conflicts of interest to declare.

References

Allen JF (2002) Photosynthesis of ATP—electrons, proton pumps, rotors, and poise. Cell 110:273–276

Allen JF (2003) Cyclic, pseudocyclic and noncyclic photophosphorylation: new links in the chain. Trends Plant Sci 8:15–19

Arnon DI (1959) Conversion of light into chemical energy in photosynthesis. Nature 184:10–21

Asada K (1999) The water-water cycle in chloroplasts: scavenging of active oxygens and dissipation of excess photons. Annu Rev Plant Biol 50:601–639

Asada K, Kiso K, Yoshikawa K (1974) Univalent reduction of molecular oxygen by spinach chloroplasts on illumination. J Biol Chem 249:2175–2181

Avenson TJ, Cruz JA, Kanazawa A, Kramer DM (2005) Regulating the proton budget of higher plant photosynthesis. Proc Natl Acad Sci USA 102:9709–9713

Badger MR, von Caemmerer S, Ruuska S, Nakano H (2000) Electron flow to oxygen in higher plants and algae: rates and control of direct photoreduction (Mehler reaction) and rubisco oxygenase. Philos Trans R Soc B 355:1433–1446

Baker NR (2008) Chlorophyll fluorescence: a probe of photosynthesis in vivo. Annu Rev Plant Biol 59:89–113

Baker NR, Harbinson J, Kramer DM (2007) Determining the limitations and regulation of photosynthetic energy transduction in leaves. Plant Cell Environ 30:1107–1125

Brestic M, Cornic G, Freyer MJ, Baker NR (1995) Does photorespiration protect the photosynthetic apparatus in French bean leaves from photoinhibition during drought stress? Planta 196:450–457

DalCorso G, Pesaresi P, Masiero S, Aseeva E, Schünemann D, Finazzi G, Joliot P, Barbato R, Leister D (2008) A complex containing PGRL1 and PGR5 is involved in the switch between linear and cyclic electron flow in Arabidopsis. Cell 132:273–285

Driever SM, Baker NR (2011) The water–water cycle in leaves is not a major alternative electron sink for dissipation of excess excitation energy when CO_2 assimilation is restricted. Plant Cell & Environ 34:837–846

Fisher N, Kramer DM (2014) Non-photochemical reduction of thylakoid photosynthetic redox carriers in vitro: relevance to cyclic electron flow around photosystem I? Biochim Biophys Acta Bioenerg 1837:1944–1954

Furbank RT, Badger MR (1983) Oxygen exchange associated with electron transport and photophosphorylation in spinach thylakoids. Biochim Biophys Acta Bioenerg 723:400–409

Golding AJ, Johnson GN (2003) Down-regulation of linear and activation of cyclic electron transport during drought. Planta 218:107–114

Gotoh E, Matsumoto M, Ogawa KI, Kobayashi Y, Tsuyama M (2010) A qualitative analysis of the regulation of cyclic electron flow around photosystem I from the post-illumination chlorophyll fluorescence transient in *Arabidopsis*: a new platform for the in vivo investigation of the chloroplast redox state. Photosynth Res 103:111–123

Grieco M, Tikkanen M, Paakkarinen V, Kangasjärvi S, Aro EM (2012) Steady-state phosphorylation of light-harvesting complex II proteins preserves photosystem I under fluctuating white light. Plant Physiol 160:1896–1910

Heber U, Walker D (1992) Concerning a dual function of coupled cyclic electron transport in leaves. Plant Physiol 100:1621–1626

Heber U, Egneus H, Hanck U, Jensen M, Köster S (1978) Regulation of photosynthetic electron transport and photophosphorylation in intact chloroplasts and leaves of *Spinacia oleracea* L. Planta 143:41–49

Hormann H, Neubauer C, Schreiber U (1994) An active Mehler-peroxidase reaction sequence can prevent cyclic PS I electron transport in the presence of dioxygen in intact spinach chloroplasts. Photosynth Res 41:429–437

Johnson GN (2011) Reprint of: physiology of PSI cyclic electron transport in higher plants. Biochim Biophys Acta Bioenerg 1807:906–911

Joliot P, Joliot A (2002) Cyclic electron transfer in plant leaf. Proc Natl Acad Sci USA 99:10209–10214

Joliot P, Béal D, Joliot A (2004) Cyclic electron flow under saturating excitation of dark-adapted *Arabidopsis* leaves. Biochim Biophys Acta Bioenerg 1656:166–176

Kanazawa A, Kramer DM (2002) In vivo modulation of nonphotochemical exciton quenching (NPQ) by regulation of the chloroplast ATP synthase. Proc Natl Acad Sci USA 99:12789–12794

Klughammer C, Schreiber U (1994) An improved method, using saturating light pulses, for the determination of photosystem I quantum yield via $P700^+$-absorbance changes at 830 nm. Planta 192:261–268

Klughammer C, Siebke K, Schreiber U (2013) Continuous ECS-indicated recording of the proton-motive charge flux in leaves. Photosynth Res 117:471–487

Kohzuma K, Cruz JA, Akashi K, Hoshiyasu S, Munekage YN, Yokota A, Kramer DM (2009) The long-term responses of the photosynthetic proton circuit to drought. Plant Cell Environ 32:209–219

Kono M, Noguchi K, Terashima I (2014) Roles of the cyclic electron flow around PSI (CEF-PSI) and O_2-dependent alternative pathways in regulation of the photosynthetic electron flow in

short-term fluctuating light in *Arabidopsis thaliana*. Plant Cell Physiol 55:990–1004
Kou J, Takahashi S, Oguchi R, Fan DY, Badger MR, Chow WS (2013) Estimation of the steady-state cyclic electron flux around PSI in spinach leaf discs in white light, CO_2-enriched air and other varied conditions. Funct Plant Biol 40:1018–1028
Kou J, Takahashi S, Fan DY, Badger MR, Chow WS (2015) Partially dissecting the steady-state electron fluxes in Photosystem I in wild-type and *pgr5* and *ndh* mutants of *Arabidopsis*. Front Plant Sci. doi:10.3389/fpls.2015.00758
Kozaki A, Takeba G (1996) Photorespiration protects C3 plants from photooxidation. Nature 384:557–560
Kramer DM, Evans JR (2011) The importance of energy balance in improving photosynthetic productivity. Plant Physiol 155: 70–78
Kramer DM, Sacksteder CA, Cruz JA (1999) How acidic is the lumen? Photosynth Res 60:151–163
Kramer DM, Johnson G, Kiirats O, Edwards GE (2004) New fluorescence parameters for the determination of Q_A redox state and excitation energy fluxes. Photosynth Res 79:209–218
Krieger-Liszkay A (2005) Singlet oxygen production in photosynthesis. J Exp Bot 56:337–346
Krieger-Liszkay A, Kós PB, Hideg É (2011) Superoxide anion radicals generated by methylviologen in photosystem I damage photosystem II. Physiol Plant 142:17–25
Laisk A, Eichelmann H, Oja V, Talts E, Scheibe R (2007) Rates and roles of cyclic and alternative electron flow in potato leaves. Plant Cell Physiol 48:1575–1588
Laisk A, Talts E, Oja V, Eichelmann H, Peterson RB (2010) Fast cyclic electron transport around photosystem I in leaves under far-red light: a proton-uncoupled pathway? Photosynth Res 103:79–95
Livingston AK, Cruz JA, Kohzuma K, Dhingra A, Kramer DM (2010) An *Arabidopsis* mutant with high cyclic electron flow around photosystem I (*hcef*) involving the NADPH dehydrogenase complex. Plant Cell 22:221–233
Miyake C (2010) Alternative electron flows (water–water cycle and cyclic electron flow around PSI) in photosynthesis: molecular mechanisms and physiological functions. Plant Cell Physiol 51:1951–1963
Miyake C, Schreiber U, Asada K (1995) Ferredoxin-dependent and antimycin A-sensitive reduction of cytochrome *b-559* by far-red light in maize thylakoids; participation of a menadiol-reducible cytochrome *b-559* in cyclic electron flow. Plant Cell Physiol 36:743–748
Miyake C, Miyata M, Shinzaki Y, Tomizawa KI (2005) CO_2 response of cyclic electron flow around PSI (CEF-PSI) in tobacco leaves—relative electron fluxes through PSI and PSII determine the magnitude of non-photochemical quenching (NPQ) of Chl fluorescence. Plant Cell Physiol 46:629–637
Miyake C, Amako K, Shiraishi N, Sugimoto T (2009) Acclimation of tobacco leaves to high light intensity drives the plastoquinone oxidation system—relationship among the fraction of open PSII centers, non-photochemical quenching of Chl fluorescence and the maximum quantum yield of PSII in the dark. Plant Cell Physiol 50:730–743
Munekage YN, Genty B, Peltier G (2008) Effect of PGR5 impairment on photosynthesis and growth in Arabidopsis thaliana. Plant Cell Physiol 49:1688–1698
Munekage Y, Hojo M, Meurer J, Endo T, Tasaka M, Shikanai T (2002) PGR5 is involved in cyclic electron flow around photosystem I and is essential for photoprotection in *Arabidopsis*. Cell 110:361–371
Nishikawa Y, Yamamoto H, Okegawa Y, Wada S, Sato N, Taira Y, Sugimoto K, Makino A, Shikanai T (2012) PGR5-dependent cyclic electron transport around PSI contributes to the redox homeostasis in chloroplasts rather than CO_2 fixation and biomass production in rice. Plant Cell Physiol 53:2117–2126
Okegawa Y, Kagawa Y, Kobayashi Y, Shikanai T (2008) Characterization of factors affecting the activity of photosystem I cyclic electron transport in chloroplasts. Plant Cell Physiol 49:825–834
Roach T, Krieger-Liszkay A (2014) Regulation of photosynthetic electron transport and photoinhibition. Curr Protein Pept Sci 15:351–362
Sacksteder CA, Kramer DM (2000) Dark-interval relaxation kinetics (DIRK) of absorbance changes as a quantitative probe of steady-state electron transfer. Photosynth Res 66:145–158
Schreiber U, Neubauer C (1990) O_2-dependent electron flow, membrane energization and the mechanism of non-photochemical quenching of chlorophyll fluorescence. Photosynth Res 25:279–293
Schreiber U, Reising H, Neubauer C (1991) Contrasting pH-optima of light-driven O_2-and H_2O_2-reduction in spinach chloroplasts as measured via chlorophyll fluorescence quenching. Z Naturforsch C Bio Sci 46:635–643
Sejima T, Takagi D, Fukayama H, Makino A, Miyake C (2014) Repetitive short-pulse light mainly inactivates photosystem I in sunflower leaves. Plant Cell Physiol 55:1184–1193
Sejima T, Hanawa H, Shimakawa G, Takagi D, Suzuki Y, Fukayama H, Makino A, Miyake C (2016) Post-illumination transient O2-uptake is driven by photorespiration in tobacco leaves. Physiol Plant 156:227–238
Shaku K, Shimakawa G, Hashiguchi M, Miyake C (2015) Reduction-induced suppression of electron flow (RISE) in the photosynthetic electron transport system of *Synechococcus elongatus* PCC 7942. Plant Cell Physiol. doi:10.1093/pcp/pcv198
Shikanai T (2007) Cyclic electron transport around photosystem I: genetic approaches. Annu Rev Plant Biol 58:199–217
Strand DD, Fisher N, Davis GA, Kramer DM (2016) Redox regulation of the antimycin A sensitive pathway of cyclic electron flow around photosystem I in higher plant thylakoids. Biochim Biophys Acta Bioenerg 1857:1–6
Suorsa M, Järvi S, Grieco M, Nurmi M, Pietrzykowska M, Rantala M, Kangasjarvi S, Paakkarinen V, Tikkanen M, Jansson S, Aro EM (2012) PROTON GRADIENT REGULATION5 is essential for proper acclimation of *Arabidopsis* photosystem I to naturally and artificially fluctuating light conditions. Plant Cell 24:2934–2948
Takagi D, Yamamoto H, Amako K, Makino A, Sugimoto T, Miyake C (2012) O_2 supports 3-phosphoglycerate-dependent O_2 evolution in chloroplasts from spinach leaves. Soil Sci Plant Nutr 58:462–468
Takagi D, Takumi S, Hashiguchi M, Sejima T, Miyake C (2016) Superoxide and singlet oxygen produced within the thylakoid membranes both cause photosystem I photoinhibition. Plant Physiol. doi:10.1104/pp.16.00246
Takahashi M, Asada K (1982) Dependence of oxygen affinity for Mehler reaction on photochemical activity of chloroplast thylakoids. Plant Cell Physiol 23:1457–1461
Takahashi M, Asada K (1988) Superoxide production in aprotic interior of chloroplast thylakoids. Arch Biochem Biophys 267:714–722
Takizawa K, Kanazawa A, Kramer DM (2008) Depletion of stromal Pi induces high 'energy-dependent' antenna exciton quenching (qE) by decreasing proton conductivity at CF_o-CF_1 ATP synthase. Plant Cell Environ 31:235–243
Tikhonov AN (2013) pH-Dependent regulation of electron transport and ATP synthesis in chloroplasts. Photosynth Res 116:511–534
Tikkanen M, Aro EM (2014) Integrative regulatory network of plant thylakoid energy transduction. Trends Plant Sci 19:10–17
Tikkanen M, Suorsa M, Gollan PJ, Aro EM (2012) Post-genomic insight into thylakoid membrane lateral heterogeneity and redox balance. FEBS Lett 586:2911–2916

Trouillard M, Shahbazi M, Moyet L, Rappaport F, Joliot P, Kuntz M, Finazzi G (2012) Kinetic properties and physiological role of the plastoquinone terminal oxidase (PTOX) in a vascular plant. Biochim Biophys Acta Bioenerg 1817:2140–2148

von Caemmerer S (2000) Biochemical models of leaf photosynthesis. CSIRO publishing, Collingwood, pp 1–165

von Caemmerer S, Farquhar GD (1981) Some relationships between the biochemistry of photosynthesis and the gas exchange of leaves. Planta 153:376–387

Wang C, Yamamoto H, Shikanai T (2014) Role of cyclic electron transport around photosystem I in regulating proton motive force. Biochim Biophys Acta Bioenerg. doi:10.1016/j.bbabio.2014.11.013

Yamamoto H, Shikanai T (2013) In planta mutagenesis of Src homology 3 domain-like fold of NdhS, a ferredoxin-binding subunit of the chloroplast NADH dehydrogenase-like complex in *Arabidopsis* A conserved arg-193 plays a critical role in ferredoxin binding. J Biol Chem 288:36328–36337

Yamori W, Shikanai T, Makino A (2015) Photosystem I cyclic electron flow via chloroplast NADH dehydrogenase-like complex performs a physiological role for photosynthesis at low light. Sci Rep. doi:10.1038/srep13908

Yamamoto H, Peng L, Fukao Y, Shikanai T (2011) An Src homology 3 domain-like fold protein forms a ferredoxin binding site for the chloroplast NADH dehydrogenase-like complex in *Arabidopsis*. Plant Cell 23:1480–1493

Zivcak M, Brestic M, Kunderlikova K, Sytar O, Allakhverdiev SI (2015a) Repetitive light pulse-induced photoinhibition of photosystem I severely affects CO_2 assimilation and photoprotection in wheat leaves. Photosynth Res 126:449–463

Zivcak M, Brestic M, Kunderlikova K, Olsovska K, Allakhverdiev SI (2015b) Effect of photosystem I inactivation on chlorophyll a fluorescence induction in wheat leaves: does activity of photosystem I play any role in OJIP rise? J Photochem Photobiol B. doi:10.1016/j.jphotobiol.2015.08.024